Radiological approach for Discrimination of Benign from Malignant Vertebral Compression Fractures

An Essay
Submitted in partial fulfillment of the requirements for M.Sc degree in Diagnostic Radiology

By:

Anne Abd Elaziz Saeed Elaidy
M.B., B.CH

Supervised by:

Proff. Dr Amany Emad Eldin
Professor of Diagnostic Radiology
Ain Shams University

Dr. Remon Zaher
Lecturer of Diagnostic Radiology
Ain Shams University

Faculty of medicine
Ain Shams University
2013

Acknowledgment

Thanks to my dear parents and my family who always provide me with love, care, support & for being always beside me throughout my life.

I would like to express my profound gratitude to Prof. Dr. Amany Emad Eldin, Professor of Radiology, Ain Shams University for her moral support, valuable supervision & advice which enabled me to fulfill this work.

I would also like to thank Dr. Remon Zaher, lecturer of Radiology, Ain Shams University for his constant help, advice and encouragement.

Anne Abd Elaziz Elaidy

List of contents

Title	Page
List of Figures	I
List of Tables	V
List of Abbreviations	VI
Introduction	VII
Aim of work	IX
Review of literature:	
Chapter 1: Related anatomical considerations	1
Chapter 2: Physical principles and technical aspects.	21
Chapter 3: Basic pathological considerations	27
Chapter 4: Radiological manifestations of vertebral compression fractures:	35
○ Role of Plain Radiography	41
○ Role of Computed Tomography	49
○ Role of MR Imaging	57
○ Scoring System using MRI and CT criteria	104
○ Role of Scintigraphy and PET Scan	109
Chapter 5: Radiological approach for vertebral compression fractures.	114
Summary	119
References	
Arabic summary	

List of figures

Figure		Page
Fig 1:	Lateral view of a typical vertebra	1
Fig 2:	Superior view of atlas	2
Fig 3:	Superior view of axis	3
Fig 4:	Superior & lateral views of thoracic vertebra	3
Fig 5:	Lumbar vertebra, lateral aspect.	4
Fig 6:	Median sagittal section through vertebrae showing discs and ligaments.	6
Fig 7:	Transverse Section, Superior View of vertebra showing intervertebral discs & ligaments	7
Fig 8:	Posterior view of the ligaments of atlanto-occipital & atlanto-axial joints.	8
Fig 9:	Anterolateral view of exposed spinal cord & meninges.	10
Fig 10:	Arterial supply to the vertebrae	11
Fig 11:	Venous drainage of the vertebral column.	12
Fig 12:	Sagittal T1 MRI of thoracic spine	13
Fig 13:	Sagittal T2 weighted MR image of the Lumbar spine .	15
Fig 14:	Sequential axial images through L5 to S1	16
Fig 15:	Axial CT of L4/L5 intervertebral disc	18
Fig 16:	Axial CT image of atlas.	19
Fig 17:	PET/CT image of the bone.	20
Fig 18:	Paget disease.	31
Fig 19:	whole-mounted specimen (H-E stain) of the lumbar spine in patient with Paget disease	32
Fig 20:	Scheuermann's Disease	33
Fig 21:	Histology demonstrates giant cell tumour	34

List of figures

Fig 22:	A. ABC, B. A Low-powered H and E stain	35
Fig 23:	A. Metastasis, B. A vertebral biopsy shows the typical clear cells of renal metastases	37
Fig 24:	Microscopy of myeloma shows sheets of plasma cells	38
Fig 25:	Histology shows small round cells and large Hodgkin's cells.	40
Fig 26	An intravertebral vacuum phenomenon on thoracolumbar spine.	42
Fig 27:	Lateral radiograph of lumbar spine of spondylilitis	43
Fig 28:	Frontal radiograph of Paget disease	44
Fig 29:	Radiograph of Sickle cell disease	44
Fig 30:	A-P radiography shows ABC	45
Fig 31:	A-P radiographs of giant cell tumour	46
Fig 32:	LCH: Lateral lumbar spine radiograph	47
Fig 33:	Lateral & AP radiograph show metastasis.	47
Fig 34:	Lateral radiograph of multiple myeloma	48
Fig 35:	CT scans of typical benign compression fracture in a woman with breast cancer	50
Fig 36:	CT scans of a typical malignant compression fracture.	51
Fig 37:	Malignant compression fracture in a 61-year-old man with hepatocellular carcinoma.	52
Fig 38:	A malignant compression fracture in a 53-year-old woman with breast cancer.	53
Fig 39:	CT of GCT	55
Fig 40:	MRI of acute benign compression fracture.	58
Fig 41:	Fluid sign in MRI of osteoporotic fracture	60
Fig 42:	CE-MRI of Osteoporotic VCF	62
Fig 43:	Sagittal STIR MR of traumatic VCF	64

List of figures

Fig 44:	T2WI & T1 +C MR of infectious collapse	65
Fig 45:	MRI of kyphotic tuberculous spondylitis	66
Fig 46:	MRI of Typical tuberculous spondylitis	67
Fig 47:	MRI of Paget disease of the spine	68
Fig 48:	Extramedullary hematopoiesis.	69
Fig 49:	MRI of Scheuermann disease	70
Fig 50:	Giant cell tumour	71
Fig 51:	Sagittal T2WI MR shows ABC	72
Fig 52:	Hemangioma with epidural extension.	73
Fig 53:	Metastasis: Sagittal T1-& T2 weighted	74
Fig 54:	MRI of malignant VCF	76
Fig 55:	Metastatic collapse	77
Fig 56:	T2 & TI + C MRI of Multiple myeloma	80
Fig 57:	Langerhans cell histiocytosis .	81
Fig 58:	Hodgkin's lymphoma,	82
Fig 59:	Multiple VCF caused by leukemia.	83
Fig 60:	DWI of the spinal osteoporotic fracture	86
Fig 61:	DWI of VCF from bronchogenic carcinoma	87
Fig 62:	STIR & ADC map of porotic fracture	86
Fig 63:	STIR & ADC map of neoplastic fracture	87
Fig 64:	MRI of traumatic VCF in a woman with breast carcinoma	91
Fig 65:	Metastasis with a history of acute trauma	92
Fig 66:	Illustration of the physical principles of in-phase/opposed-phase imaging.	94
Fig 67:	In-phase/opposed-phase imaging of metastatic melanoma	95
Fig 68:	Chronic malignant compression fracture	97
Fig 69:	Acute malignant compression fracture	98

List of figures

Fig 70:	Time intensity curve	100
Fig 71:	Five types of time intensity curve	100
Fig 72:	Multiple vertebral metastasis of thyroid cancer with pathologic fracture	102
Fig 73:	CT & MRI of metastatic VCF	106
Fig 74:	CT & MRI of Acute VCF	107
Fig 75:	Bone scan& MRI of multiple VCF	104
Fig 76:	PET/CT & MRI of benign VCF	112
Fig 77:	PET/CT & MRI of benign VCF	113
Fig 78:	Sagittal T1WI MR of T12 & L2	115
Fig 79:	Treatment algorithm for VCFs in cancer patients.	117
Fig 80:	Suggested diagram for radiological approach to differentiation between benign & malignant VCF.	118

List of tables

Table		Page
Tab. 1:	Routine spinal radiograph protocols	25
Tab. 2:	Findings of Cortical Bone of Vertebral Body in Benign and Malignant Fractures	49
Tab. 3:	Findings of Cancellous Bone of Vertebral Body in Benign and Malignant Fractures	50
Tab. 4:	Other CT Findings in Benign and Malignant Fractures	51
Tab. 5:	Significant CT Findings Suggesting Benign Fracture.	53
Tab. 6:	Significant CT Findings Suggesting Malignant Fracture	54
Tab. 7:	Incidence of the various findings (F1-F10) for the benign and malignant fracture groups	105
Tab. 8:	Simplified scoring system.	108

List of abbreviations

ABC: Aneurysmal Bone Cyst
ADC: Apparent Diffusion Coefficient
CSF: Cerebrospinal fluid
CT: Computed Tomography
DWI: Diffusion Weighted Image
EPI: Echo Planar Imaging
FDG: 2-flouro-2-deoxy-D-glucose
FSE: Fast spin echo
GCT: Giant Cell Tumor
GE: Gradient Echo
LCH: Langerhans cell Histiocytosis
MDCT: Multi Detector Computed Tomography
MM: Multiple myeloma
MRI: Magnetic Resonance Imaging
PET: Positron Emission Tomography
ROI: Region of interest
SD: Standered deviation
SIR: Signal intensity ratio
SSFP: Steady State Free Precession
SSFSE: Single Shot Fast Spin Echo
SUV: Standardized uptake value
TIC: Time Intensity Curve
TSE: Turbo spin echo
VB: vertebral body
VCF: Vertebral Compression fracture
WI: Weighted Image

Introduction

Benign vertebral lesions occur in approximately one third of cancer patients, while metastatic vertebral lesions account for 39% of bony metastases in patients with primary neoplasm. ***(Bhugaloo et al., 2006)***.

Correct diagnosis for malignant and benign vertebral compression fractures can be problematic, but it has important prognostic and therapeutic implications.***(Tokuda et al., 2011).***

This is especially so in the elderly patients who are predisposed to benign compression fracture caused by osteoporosis. ***(Bhugaloo et al., 2006)***.

Benign fractures are caused by osteoporosis and/or trauma, while malignant fractures are caused by metastatic bone tumors, multiple myeloma, and malignant lymphoma. ***(Ogura et al., 2012).***

Symptoms and signs of both types of fracture may be nonspecific and the only complaint may be back pain. ***(Fu et al., 2004).***

Traditionally, radiography, CT, and bone scintigraphy have been used in the evaluation of vertebral compression fractures. However, these techniques are often inadequate for identifying the cause of compression fractures. ***(Cho and Chang, 2011).***

But in today's clinical environment, the specific discrimination between benign and malignant vertebral compression fractures relies heavily on MR imaging features. ***(Bhugaloo et al., 2006)***.

Magnetic resonance imaging (MRI) is highly useful for detecting diseases of the bone marrow, and has become the imaging modality of choice for metastatic bone marrow disease. ***(Ogura et al., 2012).***

In the last decade, a myriad of MR pulse sequences have been used for vertebral DWI. They each have their own advantages and disadvantages. ***(Rumpel et al., 2012).***

Discrimination based on the signal intensity ratio (SIR) of opposed-phase/in-phase was reported to be useful for differential diagnosis between malignant and benign vertebral compression fracture. ***(Ogura et al., 2012).***

High-resolution CT using multi-detector row can provide many useful signs for differentiation between benign and malignant vertebral compression fractures, and its diagnostic ability is sufficient for clinical use ***(Kutoba et al., 2005)***.

By combining the findings common to MRI and CT scans of vertebral fractures, a simple scoring system was advised. This scoring system was found to enhance the accuracy of imaging diagnosis of fractures caused by benign or malignant spinal lesions ***(Yuzawa et al., 2005)***.

In cases in which MR imaging findings are not diagnostic, FDG-PET/CT can give additional information. This modality is a useful for differentiating malignant from benign VCFs because it has high sensitivity and is semiquantitative. ***(Cho and Chang, 2011).***

Aim of the work

This essay is an attempt to spot light the radiological approach for distinction of various causes of benign & malignant spine collapse, hoping to increase the diagnostic accuracy with the rapidly advancing science.

Chapter 1: Related anatomical considerations of the spine

The vertebral column is made of 33 vertebrae: 7 cervical, 12 thoracic, 5 lumbar, 5 sacral (fused) and 4 coccygeal (fused).

The spine of the fetus is flexed in a smooth C shape. This is referred to as the 'primary curvature' and is retained in the adult in the thoracic and sacrococcygeal areas. Secondary extension results in lordosis - known as the 'secondary curvature' - of the cervical and lumbar spine ***(Ryan et al., 2007).***

Gross Anatomy

A. The Osseous Anatomy:

A Typical vertebra:

It has a vertebral body anteriorly and a neural arch posteriorly which consists of pedicles laterally and of laminae posteriorly .The pedicles are notched superiorly and inferiorly so that adjoining pedicles are separated by an intervertebral foramen ***(Ryan et al., 2007).*** **(Fig. 1).**

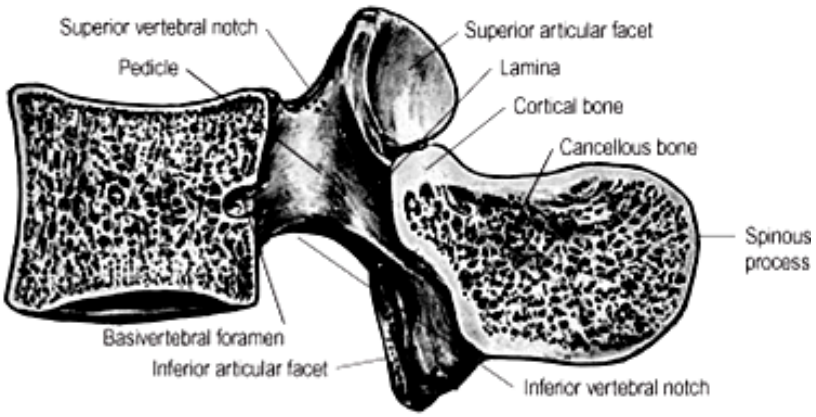

Fig.1. Lateral view of a typical vertebra ***(Standring et al., 2008).***

A transverse process arises at the junction of the pedicle and the lamina and extends laterally on each side. The laminae fuse posteriorly as the spinous process. The part of the lamina between the superior and inferior articular facets on each side is called the pars interarticularis. Articular processes project superiorly and inferiorly from each lamina ***(Ryan et al., 2007).***

I. The cervical vertebrae:

➢ Typical cervical vertebra:

Each characterized by bifid transverse processes, bifid spinous processes. All have large vertebral foramina, transverse foramina for transmission of the vertebral artery and vein (except C7), and grooves on the superior surfaces of the transverse processes for transmission of the spinal nerves ***(McKinnis, 2010).***

➢ The Atlas-C1:

It lacks both a body and a spinous process. It is composed of anterior and posterior arches united by lateral masses ***(Daffner, 2011).***

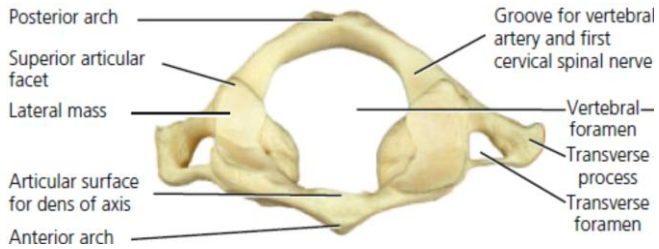

Fig. 2. Superior view of atlas (Donovan.A & Schweitzer.M, 2012).

The anterior arch of has a tubercle on its anterior surface and a facet posteriorly for articulation with the odontoid process. The posterior arch is grooved behind the lateral mass by the vertebral artery ***(Ryan et al., 2007).*** **(Fig. 2)**.

The lateral masses support large, concave facets that articulate with the occipital condyles. The inferior facets articulate with the superior facets of C2 ***(McKinnis, 2010).***

➢ The Axis-C2:

The odontoid process, represents the body of the atlas, it has a large lateral mass on each side Sloping articular facets for articulation in the atlantoaxial joint. ***(Ryan et al., 2007).*** **(Fig. 3).**

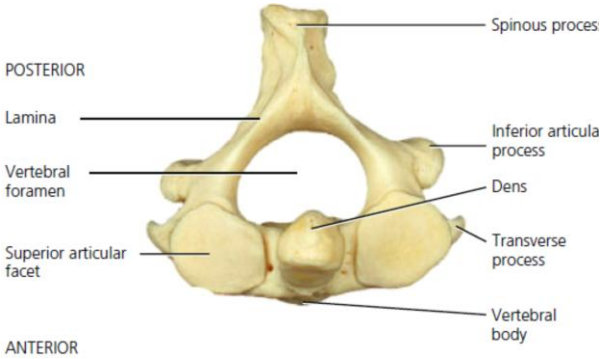

Fig. 3. Superior view of axis.***(Donovan. & Schweitzer, 2012).***

➢ The vertebra prominens-C7:

Its name is derived from its long, easily felt, non bifid spine. Its foramen transversarium is small or absent and usually transmits only vertebral veins ***(Ryan et al., 2007).***

II. The thoracic vertebrae:

These have articular facets on the lateral aspects of the vertebral bodies for articulation with the ribs. Articular facets are also found on the anterior surface of the transverse processes for the costotransverse articulations ***(Ryan et al., 2007).(Fig. 4).***

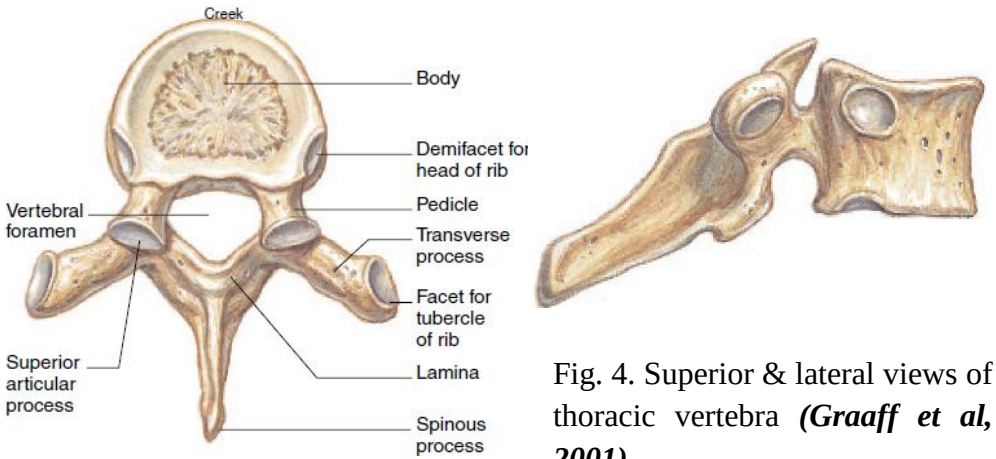

Fig. 4. Superior & lateral views of thoracic vertebra ***(Graaff et al, 2001).***